ELSEVIER

Polymer 42 (2001) 775–792

polymer

www.elsevier.nl/locate/polymer

A phenomenological study of the hot-tool welding of thermoplastics Part 3. Polyetherimide

Vijay K. Stokes*

GE Corporate Research and Development, Schenectady, NY 12301, USA

Received 5 January 2000; received in revised form 10 May 2000; accepted 16 May 2000

Abstract

A hot-tool welding machine was used to study the weldability of polyetherimide, a high-temperature amorphous thermoplastic. Weld strength data are reported for two specimen thicknesses. In these experiments, the outflow in the melting phase was controlled by means of stops, the thickness of the molten film was controlled by the heating time, and the outflow during the final joining phase was also controlled by displacement stops. Strength data for butt welds are reported for a series of tests in which the hot-tool surface temperatures, the heating times, and the displacement stop positions were varied, but the pressure was not. Within the range of the weld process parameters investigated, the highest weld strength achieved was of the order of 85% of the base strength of the material. This is lower than the 100% weld strength that can be achieved in this material by vibration welding.

Keywords: Hot-tool welding; Polyetherimide; Vibration welding

1. Introduction

Because of the increasing use of thermoplastics and thermoplastic composites in load-bearing applications, welding methods are becoming important for part cost reduction. Hot-tool welding is a widely used technique in which the surfaces to be joined are brought to the "melting temperature" by direct contact with a heated metallic tool. In some cases, such as in joining of plastic pipes, the surfaces to be joined are flat, so that the tool is a hot plate. However, in many applications, such as in automotive headlamps and rear lights, doubly curved joint interfaces require complex tools that allow the hot surfaces to match the contours of the joint interface. Applicability to complex geometries is one of the major advantages of this process.

This paper is the third in a series on hot-tool welding of thermoplastics. The hot-tool welding process is described in detail in Part 1 of this paper, which presents a comprehensive phenomenological study of the hot-tool welding of the amorphous polymer BPA polycarbonate (PC) [1]. Part 2 of the paper addresses the weldability of unfilled and glass-filled poly(butylene terephthalate) (PBT), a semi-crystalline polymer [2]. In addition to establishing the terminology, these two papers include comprehensive lists of references on hot-tool welding, including those on the weldability of other thermoplastics. As such, in this paper, only papers pertinent to the study reported in this paper are cited.

This paper examines the hot-tool weldability of unfilled polyetherimide (PEI), a high-temperature amorphous thermoplastic with a glass transition temperature of 215°C. A dual platen hot-tool welding machine with displacement control, in which the temperatures of the two hot-tool surfaces can be independently controlled, was used to study the weldability of this material. In these experiments, the outflow in the melting phase was controlled by means of stops, the thickness of the molten film was controlled by the heating time, and the outflow during the final joining phase was also controlled by displacement stops. Strength data for butt welds are reported for two specimen thicknesses for a series of tests in which the hot-tool surface temperatures, the heating times, and the displacement stop positions were varied, but the pressure was not. The effects of the large number of welding parameters were explored mainly by conducting one test per test condition studied; such data do not provide information on the variability in the weld strength at each test condition. The variability in the data were then studied through repeat tests at the near optimum conditions established by the single tests. It is shown that high weld strengths can be achieved in PEI.

* Tel.: +1-518-387-5157; fax: +1-518-387-7006.
E-mail address: stokes@crd.ge.com (V.K. Stokes).

0032-3861/01/$ - see front matter
PII: S0032-3861(00)00395-5

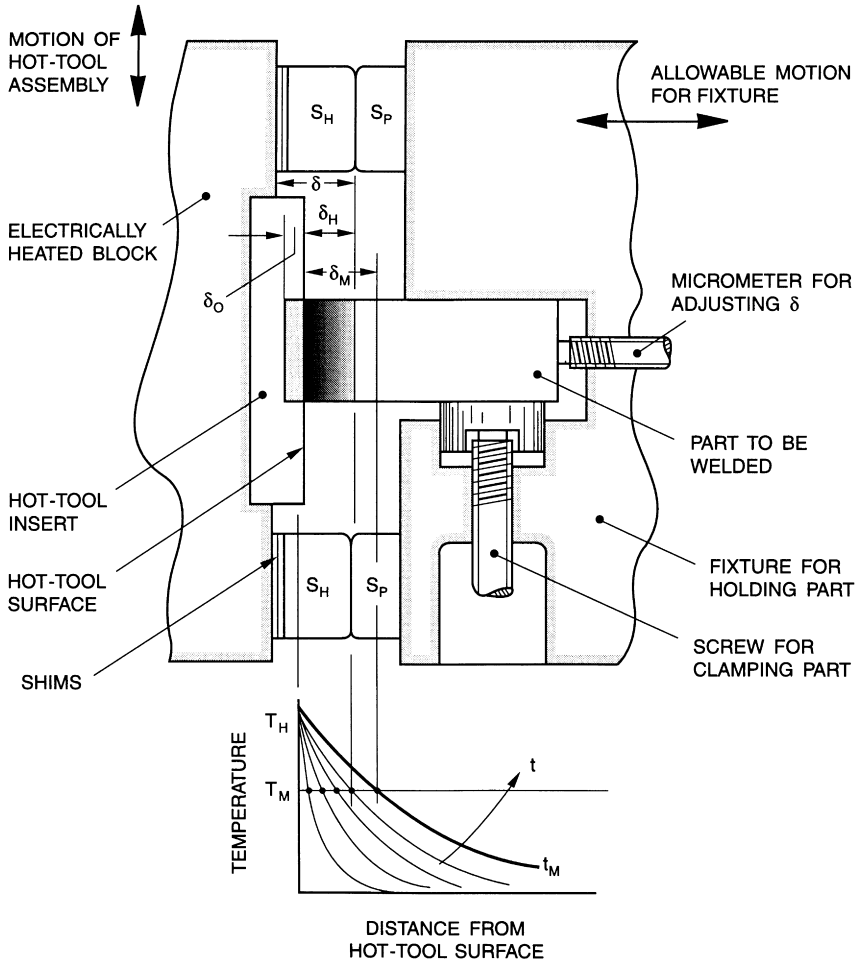

Fig. 1. Schematic diagram showing geometric parameters for displacement-controlled hot-tool welding using mechanical stops.

2. Displacement controlled welding

The essential parts of a displacement controlled welding machine consist of the hot-tool assembly having two exposed hot surfaces, two fixtures for holding the parts to be welded, means for bringing the parts in contact with the hot surfaces and then bringing the molten surfaces together to form the weld, and adequate timing and displacement controls. The mechanics of the hot-tool welding process using mechanical stops to effect displacement control can be described by means of the schematic in Fig. 1. The left-hand side shows one half of the hot-tool assembly, comprising an electrically heated block on which interchangeable hot-tool inserts can be mounted. The hot-tool assembly has mechanical stops S_H, the surfaces of which are offset from the hot-tool surface by a distance δ_H. The hot-tool assembly can be moved in and out of the configuration shown in the figure along the direction indicated.

The part to be welded is gripped in a fixture (right-hand side of figure) that can be moved to and fro in a direction at right angles to the allowable motion for the hot-tool assembly. This fixture has mechanical stops S_P that are aligned with the hot-tool stops S_H.

For welding, the fixture is moved to bring the part into contact with the hot-tool surface, and a pressure is applied to maintain this contact. Heat transfer raises the temperature of the part and the resulting thermal expansion causes a small rightward (away from the hot-tool surface) motion in the part and fixture. When the surface temperature reaches the melting point of the plastic, the externally applied pressure causes the molten material to flow laterally outward, thereby inducing a leftward motion of the part. The decrease in the part length caused by the outflow of molten material is called the penetration η, which for this phase is the part displacement from the instant of contact, and weld time is measured from this instant.

Initially, when the surface begins to melt, very little flow occurs and the molten film thickens. The flow or penetration rate begins to increase with time. The penetration (or part motion) will not change after the part stops S_P come into contact with the hot-tool stops S_H, as shown in Fig. 1. Let the elapsed time from the instant that the part touches the

hot-tool surface to the instant when the stops come into contact be t_0, and let the corresponding penetration, the *melt penetration*, be $\eta = \delta_0$ (Fig. 1). This thickness of material will melt and flow out laterally to form a part of the weld "bead." Continuing contact with the hot-tool surface after time t_0 will cause the molten layer to thicken with time. During this phase, there will be no additional penetration. However, with increasing time, thermal expansion in the portion of the part heated by conduction will cause more material to flow out, thereby resulting in an apparent increase in δ_0. Let the duration of this film buildup phase be t_M and let the thickness of the molten layer be δ_M as shown. In the changeover phase, the parts are pulled away from the hot-tool, the hot-tool is retracted, and the molten surfaces are brought into contact, thereby initiating the joining phase. Let the duration of this changeover phase be t_c. After the molten surfaces touch, the applied joining pressure squeezes out the molten material laterally, resulting in a further penetration. During this squeezing motion, heat transfer from the melt results in a cooling and in an eventual solidification of the melt.

If $\delta_M < \delta_H$, the part stops S_P cannot come into contact, so that part dimensions cannot be controlled. However, if $\delta_M > \delta_H$, the material in the molten layer will continue to be squeezed out until the stops S_P come into contact, after which part motion will stop and the melt will solidify without further motion. For dimensional control, t_M should be large enough to ensure that $\delta_M > \delta_H$. For this case, the total penetration on each of the halves being welded will be $\delta = \delta_0 + \delta_H$, so that the overall (warm) part length will decrease by 2δ, if thermal expansion effects are neglected. Let the initial lengths of the parts before welding be l_1 and l_2, and let the length of the welded part be l_0. Then, $\Delta l = l_1 + l_2 - l_0$ is the thickness of the material that flowed out into the weld bead. If the stops come into contact during the joining phase (for which $\delta_M > \delta_H$) and thermal expansion effects are neglected, then the expected change in length should be 2δ. However, if $\delta_M < \delta_H$, then the stops will not come into contact and the change in length should be less than 2δ. Thus, *if* thermal expansion effects are neglected, $\Delta\eta = 2\delta - \Delta l$ is a measure for whether or not the stops come into contact: stops do and do not contact when $\Delta\eta = 0$ and $\Delta\eta > 0$, respectively. However, thermal expansion at the heated ends of the specimens would increase Δl and, in the case in which stops contact, could result in negative values of the differential penetration $\Delta\eta$. Thus, a larger Δl could result from thermal expansions both in Phase 1 (an apparent increase in δ_0) and during the joining phase. Let the thermal expansion of the specimen be δ_T, so that the effective change in length would be $2(\delta + \delta_T)$. Then, $\Delta\eta_T = 2(\delta + \delta_T) - \Delta l$ will be a better measure for whether or not stops come into contact.

An estimate for this temperature-induced length increase δ_T is [1]

$$\delta_T = \frac{2\delta}{\sqrt{\pi}}(T_H - T_a)\sqrt{\kappa t} \quad (1)$$

in which the thermal diffusivity κ the thermal expansion coefficient α have been assumed to be constant (temperature independent).

This constant-property approximation requires representative values for κ and α. The density of PEI decreases continuously from 1.27 g cm^{-3} at 20°C to 1.22 g cm^{-3}·at 215°C. After that, the density decreases from 1.22 g cm^{-3} at 215°C to 1.08 g cm^{-3} at 455°C. The average density between 20 and 215°C is 1.25 g cm^{-3}, and that between 215 and 455°C is 1.15 g cm^{-3}. The average 1.20 g cm^{-3} of these two densities at will be used as the mean density for calculating the mean thermal diffusivity. Using a thermal conductivity of 0.29 W °C^{-1}, and a specific heat of 1500 J kg^{-1} °C^{-1}, then gives a mean thermal diffusivity of 0.16 mm^2 s^{-1}. The thermal expansion coefficient of PEI decreases continuously from 0.49×10^{-4} °C^{-1} at 20°C to 0.48×10^{-4} °C^{-1} at 200°C. It undergoes a large change near the glass transition temperature, $T_g = 215$°C, of PEI. Above T_g, α decreases from 1.9×10^{-4} °C^{-1} at 215°C to 1.6×10^{-4} °C^{-1} at 455°C. Since the focus here is on obtaining an *estimate* for δ_T, an upper bound for δ_T will be obtained by using a constant thermal expansion coefficient of $\alpha = 1.7\times10^{-4}$°C^{-1}, the mean of the values at 215 and 455°C. By assuming a constant κ of 0.16 mm^2 s^{-1} and a constant α of 1.7×10^{-4} °C^{-1}, the expression in Eq. (1) reduces to $\delta_T = 0.767\times10^{-4}(T_H - T_a)\sqrt{t}$ mm. From this expression, estimates for δ_T at different hot-tool temperatures and heating times, for an ambient temperature of $T_a =$ 20°C, are listed in Table 1.

As the molten material cools, thermal contraction generates tensile stress in the solidifying material. This stress field can affect the residual stresses induced by the nonhomogeneous cooling. Clearly, δ_0 by itself does not contribute to the welding that occurs during the joining phase; this material just flows outward into the bead. A small value of δ_0 is required to compensate for part surface irregularities and for ensuring that contaminated surface layers flow out before the

Table 1
Estimates for thermally induced length increases in PEI specimens at different hot-tool temperatures and heating times, for an ambient temperatures of $T_a = 20$°C

Hot-tool temperature (°C)	Estimate for thermally induced expansion δ_T (10^{-2} mm)		
	$t_H = 10$ s	$t_H = 15$ s	$t_H = 20$ s
305	7	8	10
320	7	9	10
335	8	9	11
350	8	10	11
365	8	10	12
380	9	11	12
395	9	11	13
410	9	12	13
425	10	12	14
440	10	12	14
455	11	13	15

joining phase. The *weld penetration*, the penetration $\eta_j = \delta_H$ during the joining phase, is controlled by the machine setting δ_H (Fig. 1). Let the duration of the joining (or welding) phase, from the instant the molten surfaces touch to the instant the solidified weld is released, be t_w. Then the total welding time is given by $t_T = t_0 + t_M + t_c + t_w$. Clearly, t_c should be as small as possible.

3. Test procedure

All the test data in this paper were obtained from 3.2- and 6.2-mm-thick specimens cut from 152 × 203-mm injection-molded plaques of PEI (ULTEM® 1000). The edges of each specimen were machined to obtain rectangular blocks of size 76.2 × 25.4-mm × thickness for assuring accurate alignment of the surfaces during butt welding along the 25.4-mm × thickness edges.

All the welds were made on a commercially available (Hydra-Sealer Model VA-1015, Forward Technology Industries, Inc.) dual platen hot-tool welding machine in which the temperatures of the two hot-tool surfaces can be independently controlled. On this machine, the offset δ_H, called the weld penetration, of the hot-tool stop S_H from the hot-tool surface (Fig. 1) can only be changed by inserting shims between the electrically heated hot-tool block and the stops, which are fastened to the block surface by means of screws. All the data in this paper were obtained at three weld penetrations of $\delta_H = 0.25$, 0.66, and 0.91 mm, and two melt penetrations of $\delta_0 = 0$ and 0.13 mm.

The weld specimens are pneumatically gripped in special fixtures that accurately align the specimens during the welding cycle. Each grip is provided with a micrometer that can be used to accurately set the distance δ by which each specimen protrudes beyond the stops S_P, any variations in the lengths of the specimens can easily be compensated for. In this machine, the times t_0 and t_M cannot be resolved, only the total heating time $t_H = t_0 + t_M$ can be set and measured. However, for $\delta_0 \ll \delta_H$, t_0 should be much smaller than t_M. The changeover time t_c, from the instant the heated specimens are pulled back from the hot-tool to the instant the molten films are brought back into contact, can be changed by changing the decelerating springs and the air pressure on the displacement pistons. However, the possible range of variation is quite small. In the tests reported in this paper, a fixed changeover time t_c of about 1.24 s was used; the corresponding average changeover velocity seen by the specimen molten surfaces was about 118 mm s^{-1}. The welding, or joining, time t_w, measured from the instant the molten films are brought into contact to the instant the (solidified) welded parts are released, can be preset in this machine.

One limitation of this machine is the lack of adequate pressure control at the weld interface. For 3.2- and 6.2-mm-thick welds (specimen cross sections of thickness × 25.4 mm), the nominal weld pressures (based on the air pressure and the piston cross-sectional area) were 6.9 and 3.6 MPa, respectively.

An important characteristic of the hot-tool surface is the extent to which molten polymer tends to stick to the surface. Residue left behind can affect the quality of subsequent welds [1,2]. Because PEI requires weld temperatures in the range of 350–450°C, an uncoated metal insert, made of a high-conductivity copper–nickel–silicon–chromium alloy (Ampco 940, about 96% of which is copper), was used for all the tests reported in this paper. To eliminate the effects of residues resulting from the tendency of the melt to stick to the surface, a copper scraper was used to clean the hot-tool surface after each test.

In contrast to the weld studies on PC and PBT [1,2], the texture of the melt surface of PEI just before the final joining phase, which can be expected to affect weld quality, was not studied.

The test procedure for determining weld strength is as follows: first, the hot-tool surfaces are allowed to attain the desired surface temperatures. After accurately measuring their lengths, the weld specimens are mounted on the specimen holding fixtures and the micrometer settings are adjusted to obtain desired values of the overhang δ. The heating time t_H and the welding time t_w are set and the machine is cycled to effect the weld. The weld results in a 152.4 × 25.4-mm × thickness bar. After sufficient cooling, the length of the bar is accurately measured with a micrometer. The difference Δl of this final length from the combined lengths of the unwelded specimen pairs determines the thickness of the material that actually flowed out, i.e. the actual penetration, which can be compared with 2δ. The rectangular bar is routed down to a standard ASTM D638 tensile test specimen with a butt joint at its center [3]. The tensile bar, which has a transverse butt weld at mid length, is then subjected to a constant displacement rate tensile test in which the strain across the weld is monitored with an extensometer. In this way the average failure strain across the weld over a 25.4-mm gauge length can be monitored. All the weld strength tensile tests reported in this paper were done at a nominal strain rate of 0.01 s^{-1}.

The weld flash, or "bead," was not removed, and the weld strengths were obtained by dividing the load at failure by the original cross-sectional area of the specimen. Because large local deformations at the weld interface increase the local cross-sectional area, the true failure stress (based on the actual local cross-sectional area) will be smaller than the nominal stress (based on the original cross-sectional area) reported in this paper [4].

Furthermore, the 25.4-mm gauge-length extensometer can grossly underestimate the local strain in the failure region once strain localization sets in, so that the significance of the reported failure strains ε_0 should be interpreted with care. These values only represent the lower limit of the failure strain at the weld.

Of importance are deposits on the hot-tool surfaces that could affect the temperature and surface texture seen by the

Table 2
Strength and ductility data for hot-tool welds of 3.2-mm-thick PEI specimens, at a strain rate of $\dot{\varepsilon} = 0.01\ s^{-1}$, as functions of the hot-tool temperature and the heating time, for two weld penetrations of 0.25 and 0.66 mm. The melt penetration was maintained at 0.13 mm, and the seal time was kept constant at 10 s

Hot-tool temperature (°C)	Heating time (s)	Weld strength (MPa)		Relative weld strength[a] (%)		Failure strain[b] (%)		Δl (mm)		Differential penetration $\Delta\eta$ ($\Delta\eta_T$) (10^{-2} mm)	
		$\delta_H = 0.25$ mm	$\delta_H = 0.66$ mm	$\delta_H = 0.25$ mm	$\delta_H = 0.66$ mm	$\delta_H = 0.25$ mm	$\delta_H = 0.66$ mm	$\delta_H = 0.25$ mm	$\delta_H = 0.66$ mm	$\delta_H = 0.25$ mm	$\delta_H = 0.66$ mm
305	10	9.5	–	9	–	0.24	–	0.78	–	−2 (12)	–
320	10	19.9	17.8	18	16	0.57	0.51	0.87	1.14	−11 (3)	44 (58)
335	10	26.8	14.3	24	13	0.84	0.39	0.94	1.25	−18 (−2)	33 (49)
350	10	42.7	18.5	38	17	1.37	0.54	0.94	1.50	−18 (−2)	8 (24)
365	10	46.5	32.7	42	29	1.46	0.98	0.96	1.58	−20 (−4)	0 (16)
380	10	45.4	76.7	41	69	1.44	2.71	1.06	1.61	−30 (−12)	−3 (15)
395	10	44.4	78.6	40	70	1.41	2.86	0.98	1.70	−22 (−4)	−12 (6)
410	10	39.9	75.7	36	68	1.28	2.71	1.07	1.53	−31 (−13)	5 (23)
425	10	–	75.1	–	67	–	2.69	–	1.54	–	4 (24)
440	10	–	79.9	–	72	–	2.74	–	1.66	–	−8 (12)
455	10	–	73.0	–	65	–	2.61	–	1.77	–	−19 (3)
305	15	16.1	–	14	–	–	–	0.84	–	−8 (8)	–
320	15	25.4	15.1	23	14	0.74	0.44	0.90	1.35	−14 (4)	23 (41)
335	15	36.6	27.4	33	25	1.20	0.81	0.99	1.39	−23 (−5)	19 (37)
350	15	37.1	65.9	33	59	1.15	2.25	0.96	1.59	−20 (0)	−1 (19)
365	15	37.2	79.1	33	71	1.18	2.86	1.00	1.67	−24 (−4)	−9 (11)
380	15	40.7	76.5	36	69	1.30	2.78	1.06	1.71	−30 (−8)	−13 (9)
395	15	37.2	66.5	33	60	1.20	2.27	1.09	1.72	−33 (−11)	−14 (8)
410	15	32.2	51.4	29	46	1.08	1.76	1.17	1.52	41 (−17)	6 (30)
425	15	–	34.6	–	31	–	1.15	–	1.62	–	−4 (20)
440	15	–	53.0	–	47	–	1.90	–	1.66	–	−8 (16)
455	15	–	44.1	–	40	–	1.72	–	1.73	–	−15 (11)
305	20	21.1	–	19	–	0.61	–	0.92	–	−16 (4)	–
320	20	30.5	23.8	27	21	0.98	0.68	0.94	1.40	−18 (2)	18 (38)
335	20	33.5	67.0	30	60	1.04	2.27	0.95	1.42	−19 (3)	16 (38)
350	20	32.2	79.4	29	71	1.01	2.81	1.04	1.59	−28 (−6)	−1 (21)
365	20	27.5	67.1	25	60	0.85	2.34	1.07	1.73	−31 (−7)	−15 (9)
380	20	35.2	55.8	32	50	1.13	1.90	1.12	1.70	−36 (−12)	−12 (12)
395	20	25.7	46.2	23	41	0.84	1.59	1.08	1.73	−32 (−6)	−15 (11)
410	20	23.2	32.5	21	29	0.82	1.12	1.05	1.55	−29 (−3)	3 (29)
425	20	–	24.9	–	22	–	0.88	–	1.60	–	−2 (26)
440	20	–	35.2	–	32	–	1.28	–	1.71	–	−13 (15)
455	20	–	37.0	–	33	–	2.12	–	1.72	–	−14 (16)

[a] $\sigma_0 = 111.6$ MPa.
[b] $\varepsilon_0 = 7.1\%$.

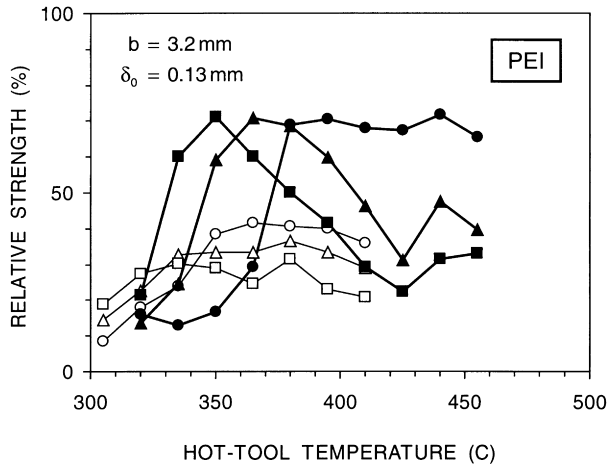

Fig. 2. Weld strength of 3.2-mm-thick PEI as a function of the hot-tool temperature, with the heating time as parameter. Circles, triangles, and squares correspond, respectively, to heating times of 10, 15, and 20 s. Open symbols (connected by thin lines) and solid symbols (connected by thick lines) correspond to weld penetrations and 0.25 and 0.66 mm, respectively. The melt penetration was maintained at 0.13 mm and the seal time was 10 s.

specimen. Also, debris from an unclean surface could be transferred to the molten surface — the resulting contamination could affect weld strength. The hot-tool surfaces were examined and cleaned after each test. Cleaning was more difficult at higher hot-tool temperatures and longer heating times.

4. Weld strength of PEI

In this paper, the total time $t_H = t_0 + t_M \approx t_M$ for which the specimen is in contact with the hot-tool will be referred to as the heating time; melt penetration will refer to the distance δ_0 (Fig. 1); weld penetration will refer to the distance δ_H; and the time t_w will be referred to as the seal time. For the data in this paper, the process parameters were varied as follows: hot-tool temperatures from $T_H = 305$ to 455°C; heating times of $t_H = 10$, 15, and 20 s; two melt penetrations of $\delta_0 = 0$ and 0.13 mm; three weld penetrations of $\delta_H = 0.25$, 0.66, and 0.91 mm; and a constant seal time of $t_w = 10$ s. The weld specimens were cut from 3.2- and 6.2-mm-thick injection-molded PEI plaques.

4.1. Weld strength of 3.2-mm-thick PEI specimens

Strength and ductility data for 3.2-mm-thick PEI specimens, at a nominal strain rate of 0.01 s^{-1}, as functions of the hot-tool temperature and the heating time, are listed in Table 2. The PEI specimens had a yield strength of 111.6 MPa and a yield strain of 7.1%. The melt penetration was maintained at 0.13 mm, the seal time was kept constant at 10 s, and two weld penetrations of 0.25 and 0.66 mm were used. The first column in this table shows that the hot-tool temperature was varied between 305 and 455°C. The second column shows the three heating times used (10, 15, and 20 s). For a weld penetration of 0.25 mm, columns 3, 5, 7, 9, and 11 list, respectively, the weld strength, the relative weld strength (σ_R = weld strength/strength of PEI resin), the failure strain, the change in length Δl after welding, and the differential penetrations $\Delta\eta$ and $\Delta\eta_T$. Columns 4, 6, 8, 10, and 12 list the corresponding data for a weld penetration of 0.66 mm. Note that the hot-tool temperatures for weld penetrations of 0.25 and 0.66 mm were different — 305–410 and 320–455°C, respectively.

The open symbols in Fig. 2, connected by *thin* lines, show the relative weld strength (data from Table 2) for a weld penetration of 0.25 mm as a function the hot-tool temperature for three heating times of 10, 15, and 20 s (indicated, respectively, by *open* circles, triangles, and squares). The relative weld strength is based on a resin strength of 111.6 MPa. For a heating time of $t_H = 10$ s, relative weld strengths lie in the range 9–42% for hot-tool temperatures in the range $T_H = 365$–410°C; the maximum relative strength of 42% is obtained at $T_H = 365$°C. The corresponding failure strains are in the range 0.24–1.46%. For $t_H = 20$ s, relative weld strengths ranging from 14 to 36% are obtained for $T_H = 305$–410°C; failure strain are in the range 0.7–1.3%. The maximum weld strength of 36% is obtained at $T_H = 380$°C. For $t_H = 20$ s, relative weld strengths of 19–32% are obtained for $T_H = 305$–410°C. The failure strains for this temperature range vary from 0.61 to 1.04%. Thus, for a weld penetration of 0.25 mm, relative strengths of about 40% can be attained over a hot-tool temperature window of 350–395°C for a heating time of 10 s. The attainable weld strengths at higher heating times are lower.

The filled symbols in Fig. 2, connected by *thick* lines, show the weld strength (data from Table 2) for the higher weld penetration of 0.66 mm as a function the hot-tool for three heating times of 10, 15, and 20 s (indicated, respectively, by *filled* circles, triangles, and squares). For a heating time of $t_H = 10$ s, relative weld strengths of 13–72% can be obtained in the hot-tool temperature range $T_H = 320$–455°C. The corresponding failure strains are in the range 0.5–2.9%. The relative strength is greater than 67% in the temperature range of $T_H = 380$–440°C, with a maximum relative strength of 72% at $T_H = 440$°C. In this temperature range the failure strains are greater than 2.7%. For $t_H = 15$ s, relative weld strengths of about 14–71% are obtained for $T_H = 320$–455°C-failure strain are in the range 0.4–2.9%. For $t_H = 20$ s, relative weld strengths of 21–71% are obtained for $T_H = 320$–455°C, the maximum strength being achieved at $T_H = 350$°C. The failure strains for this temperature range vary from 0.7 to 2.8%. Thus, for a weld penetration of 0.66 mm, relative strengths of about 70% can be attained over a hot-tool temperature window of 350–440°C. Clearly, the hot-tool temperature window for high strength is widest for $t_H = 10$ s.

For a melt penetration of 0.13 mm, the highest weld strengths are clearly obtained at the higher weld penetration of $\eta = 0.66$ mm, for which relative strengths of about 70%

Table 3
Strength and ductility data for hot-tool welds of 3.2-mm-thick PEI specimens, at a strain rate of $\dot{\varepsilon} = 0.01\ s^{-1}$, as functions of the hot-tool temperature and the heating time, for two melt penetrations of 0 and 0.13 mm. The weld penetration was maintained at 0.66 mm and the seal time was kept constant at 10 s

Hot-tool temperature (°C)	Heating time (s)	Weld strength (MPa)		Relative weld strength[a] (%)		Failure strain[b] (%)		Δl (mm)		Differential penetration $\Delta\eta(\Delta\eta_T)$ (10^{-2} mm)	
		$\delta_0 = 0.0$ mm	$\delta_0 = 0.13$ mm	$\delta_0 = 0.0$ mm	$\delta_0 = 0.13$ mm	$\delta_0 = 0.0$ mm	$\delta_0 = 0.13$ mm	$\delta_0 = 0.0$ mm	$\delta_0 = 0.13$ mm	$\delta_0 = 0.0$ mm	$\delta_0 = 0.13$ mm
350	10	19.2	18.5	17	17	0.57	0.54	1.13	1.50	19 (35)	8 (24)
365	10	41.0	32.7	37	29	1.30	0.98	1.21	1.58	11 (27)	0 (16)
380	10	51.5	76.7	46	69	1.73	2.71	1.37	1.61	−5 (13)	−3 (15)
395	10	93.4	78.6	84	70	3.73	2.86	1.44	1.70	−12 (6)	−12 (6)
350	15	67.8	65.9	61	59	2.40	2.25	1.24	1.59	8 (28)	−1 (19)
365	15	81.7	79.1	73	71	3.00	2.86	1.36	1.67	−4 (16)	−9 (11)
380	15	91.5	76.5	82	69	3.59	2.78	1.47	1.71	−15 (7)	−13 (9)
395	15	89.3	66.5	80	60	3.35	2.27	1.51	1.72	−19 (3)	−14 (8)
350	20	89.6	79.4	80	71	3.55	2.81	1.41	1.59	−9 (13)	−1 (21)
365	20	80.7	67.1	72	60	–	2.34	1.44	1.73	−12 (12)	−15 (9)
380	20	78.2	55.8	70	50	2.95	1.90	1.45	1.70	−13 (11)	−12 (12)
395	20	61.4	46.2	55	41	2.38	1.59	1.56	1.73	−24 (2)	−15 (11)

[a] $\sigma_0 = 111.6$ MPa.
[b] $\varepsilon_0 = 7.1\%$.

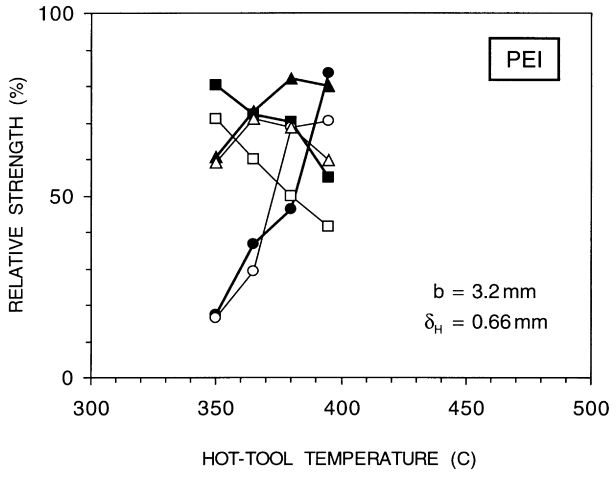

Fig. 3. Weld strength of 3.2-mm-thick PEI as a function of the hot-tool temperature, with the heating time as parameter. Circles, triangles, and squares correspond, respectively, to heating times of 10, 15, and 20 s. Open symbols (connected by thin lines) and solid symbols (connected by thick lines) correspond to melt penetrations and 0 and 0.13 mm, respectively. The weld penetration was maintained at 0.66 mm and the seal time was 10 s.

can be obtained for $T_H = 350$–$440°C$. Over this fairly wide weld process window of $T_H = 350$–$440°C$, the welds exhibit a fair amount of ductility, with failure strains in the range of 2.7–2.9%. For the lower weld penetration of 0.25 mm, the obtainable weld strengths are lower — $\sigma_R = 70\%$ over a hot-tool temperature window of 350–395°C, with a maximum of $\sigma_R = 42\%$ at $T_H = 365°C$.

Earlier, it was argued that, *if* thermal expansion effects are neglected, then the differential penetration $\Delta\eta \geq 0$, and that stops do and do not contact when $\Delta\eta = 0$ and $\Delta\eta > 0$, respectively. However, when thermal expansion at the heated ends of the specimens is accounted for, a better measure for whether or not stops come into contact is $\Delta\eta_T \geq 0$. The second last column (data for the smaller weld penetration of 0.25 mm) in Table 2 show that $\Delta\eta$ has negative values. Although the corresponding values of $\Delta\eta_T$ are larger, as expected, most of them are still negative. For the larger weld penetration of 0.66 mm, the last column in Table 2 shows that while $\Delta\eta$ is positive over a range of low hot-tool temperatures, it is still negative at higher temperatures. However, $\Delta\eta_T$ is positive over the same temperature range.

One explanation for this discrepancy would be errors in the measurements of δ_0 and the weld penetration δ_H. Instead of the two stops shown in the schematic in Fig. 1, contact is actually determined by four stops on each side. The difficulty in establishing even contact among the four stops on each side could result in errors in δ_0 and δ_H. A combined small increase of $\delta = \delta_0 + \delta_H = 0.1$ mm would make all values of $\Delta\eta_T$ greater than or equal to zero. This argument is supported by the fact that, for the same process conditions, $\Delta\eta_T$ is mostly larger for the larger weld penetration of 0.66 mm — any systematic error in the measurements would be a smaller fraction of larger settings.

The data in the last two columns of Table 2 do show the following trends that are consistent with expectations based on the underlying physics: First, at any fixed heating time t_H, in most cases $\Delta\eta_T$ decreases with increases in the hot-tool temperature T_H; this is to be expected because higher temperatures result in thicker molten layers thereby allowing for the hot-tool stops to come closer before the melt freezes off. Second, for a fixed hot-tool temperature, in most cases $\Delta\eta_T$ again decreases with increases in the melt time; this is explained by increased heating times resulting in thicker molten films.

4.1.1. Effect of melt penetration

To study the effect of the melt penetration, a limited series of tests at four hot-tool temperatures of $T_H = 350$, 365, 380, and 395°C and three heating times of 10, 15 and 20 s, were done at a melt penetration of $\delta_0 = 0$ mm and $\delta_H = 0.66$ mm. The data for these tests, in the same format as the data in Table 2, are listed in Table 3. In this table, the data for $\delta_0 = 0.13$ mm have been obtained from Table 2. For $\delta_H = 0.66$ mm, the variations of the relative weld strengths for $\delta_0 = 0$ and 0.13 mm are shown in Fig. 3 by the open and closed symbols, respectively. As before circles, triangles, and squares correspond, respectively, to melt times of 10,15, and 20 s.

A comparison of the data for these two melt penetrations shows that, except for one set of conditions ($T_H = 380°C$ and $t_H = 10$ s) the weld strength is systematically higher at the lower melt penetration. For the lower melt penetration of 0 mm, relative weld strengths higher than 80% were obtained at several process conditions: $T_H = 395°C$, $t_H = 10$ s; $T_H = 380$–$395°C$, $t_H = 15$ s; and $T_H = 350°C$, $t_H = 20$ s. The highest weld strength of 84% was obtained at $T_H = 395°C$, $t_H = 10$ s. Also, the relative weld strength is greater than 70% for $T_H = 350$–$395°C$, $t_H = 15$ s, and for $T_H = 350$–$380°C$, $t_H = 20$ s. Clearly, for this thickness of the material, at the lower melt penetration of 0 mm substantially higher weld strengths of about 84% can be obtained in comparison to a strength of about 70% for the higher melt penetration of 0.13 mm.

4.2. Weld strength of 6.2-mm-thick PEI specimens

Because tests on 3.2-mm-thick material showed that higher strengths are obtained at a higher weld penetration but a lower melt penetration, for the 6.2-mm-thick material tests were first done at a weld penetration of 0.66 mm, at two melt penetrations of 0 and 0.13 mm, and a constant seal time of 10 s. Repeatability data were also acquired for these test conditions. Then, to determine whether still higher weld strengths could be achieved by increasing the weld penetration, additional weld tests were done at weld and melt penetrations of 0.91 and 0.13 mm, respectively. In these tests, the hot-tool temperature was varied in the range of 320–455°C at intervals of 15°. Data for melt penetrations of 0.66 and 0.91 mm are compared first, after which the

Table 4
Strength and ductility data for hot-tool welds of 6.2-mm-thick PEI specimens, at a strain rate of $\dot{\varepsilon} = 0.01\ s^{-1}$, as functions of the hot-tool temperature and the heating time, for two weld penetrations of 0.66 and 0.91 mm. The melt penetration was maintained at 0.13 mm and the seal time was kept constant at 10 s

Hot-tool temperature (°C)	Heating time (s)	Weld strength (MPa)		Relative weld strength[a] (%)		Failure strain[b] (%)		Δl (mm)		Differential penetration $\Delta\eta$ ($\Delta\eta_T$) (10^{-2} mm)	
		$\delta_H = 0.66$ mm	$\delta_H = 0.91$ mm	$\delta_H = 0.66$ mm	$\delta_H = 0.91$ mm	$\delta_H = 0.66$ mm	$\delta_H = 0.91$ mm	$\delta_H = 0.66$ mm	$\delta_H = 0.91$ mm	$\delta_H = 0.66$ mm	$\delta_H = 0.91$ mm
320	10	17.8	–	16	–	0.54	–	0.37	–	121 (135)	–
335	10	29.5	34.0	26	30	0.83	1.08	0.51	0.45	107 (123)	163 (179)
350	10	38.6	48.8	35	44	1.20	1.57	0.63	0.69	95 (111)	139 (155)
365	10	43.3	70.4	39	63	1.39	2.32	0.76	0.88	82 (98)	120 (136)
380	10	41.8	63.7	37	57	1.37	2.15	1.02	1.06	56 (74)	102 (120)
395	10	48.4	60.8	43	54	1.55	2.09	1.16	1.28	42 (60)	80 (98)
410	10	52.7	70.1	47	63	1.63	2.32	1.13	1.36	45 (63)	72 (90)
425	10	56.0	86.6	50	78	1.76	2.39	1.12	1.46	46 (66)	62 (82)
440	10	85.3	86.2	76	77	3.19	2.38	1.33	1.55	25 (45)	53 (73)
455	10	81.8	81.5	73	73	2.99	2.38	1.36	1.67	22 (44)	41 (63)
320	15	25.2	–	23	–	1.10	–	0.81	–	77 (95)	–
335	15	36.5	54.7	33	49	1.19	1.98	1.06	1.13	52 (70)	95 (113)
350	15	39.5	60.7	35	54	1.19	1.98	1.06	1.13	52 (72)	95 (115)
365	15	44.9	47.2	40	42	1.39	1.57	1.20	1.34	38 (58)	74 (94)
380	15	65.3	65.4	58	59	2.12	2.30	1.31	1.48	27 (49)	60 (82)
395	15	76.8	66.5	69	60	2.69	2.06	1.30	1.77	28 (50)	31 (53)
410	15	83.0	67.3	74	60	3.08	2.32	1.41	1.90	17 (41)	18 (42)
425	15	74.8	81.3	67	73	2.77	2.41	1.27	1.96	31 (55)	12 (36)
440	15	71.2	69.4	64	62	2.48	2.35	1.41	2.02	17 (41)	6 (30)
455	15	63.7	86.7	57	78	2.23	2.30	1.45	2.07	13 (39)	1 (27)
320	20	29.7	–	27	–	0.93	–	0.85	–	73 (93)	–
335	20	29.8	63.1	27	57	0.85	2.18	1.15	1.11	43 (63)	97 (119)
350	20	48.1	65.7	43	59	1.48	2.08	1.24	1.45	34 (56)	63 (85)
365	20	82.4	60.5	74	54	2.95	2.05	1.30	1.73	28 (50)	35 (59)
380	20	84.6	65.5	76	59	3.07	2.21	1.26	1.94	32 (56)	14 (38)
395	20	80.5	91.1	72	82	2.86	2.39	1.39	1.90	19 (45)	18 (44)
410	20	71.5	94.6	64	85	2.55	2.36	1.44	2.09	14 (40)	−1 (25)
425	20	62.7	90.1	56	81	2.14	2.26	1.50	2.12	8 (36)	−4 (24)
440	20	55.3	89.3	50	80	1.87	2.38	1.46	2.17	12 (40)	−9 (19)
455	20	48.0	78.3	43	70	1.65	2.40	1.50	2.30	8 (36)	−22 (8)

[a] $\sigma_0 = 111.6$ MPa.
[b] $\varepsilon_0 = 7.1\%$.

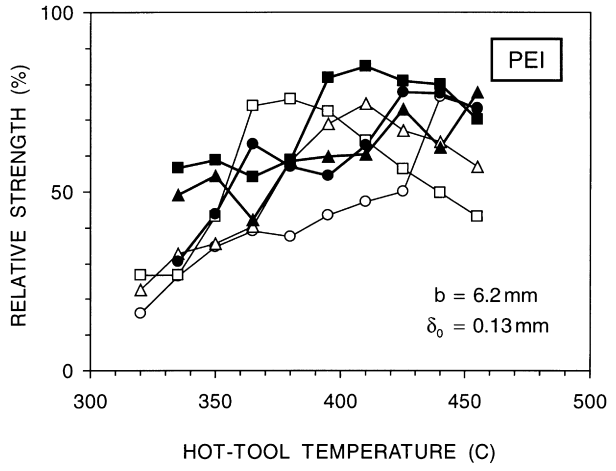

Fig. 4. Weld strength of 6.2-mm-thick PEI as a function of the hot-tool temperature, with the heating time as parameter. Circles, triangles, and squares correspond, respectively, to heating times of 10, 15, and 20 s. Open symbols (connected by thin lines) and solid symbols (connected by thick lines) correspond to weld penetrations and 0.66 and 0.91 mm, respectively. The melt penetration was maintained at 0.13 mm and the seal time was 10 s.

repeatability of data for a weld penetration of 0.66 mm is discussed.

Strength and ductility data for 6.2-mm-thick PEI specimens, at a nominal strain rate of 0.01 s^{-1}, for two weld penetrations of 0.66 and 0.91 mm, at a fixed melt penetration of 0.13 mm, as functions of the hot-tool temperature and the heating time, are listed in Table 4.

The open symbols in Fig. 4, connected by thin lines, show the weld strength (data from Table 4) for a weld penetration of 0.66 mm as a function the hot-tool temperature for three heating times of 10,15, and 20 s (indicated, respectively, by the open circles, triangles, and squares). For a heating time of $t_H = 10$ s, the relative weld strength is less than or equal to 50% except for hot-tool temperatures in the range 440–455°C. The relative weld strengths are 76 and 73% at $T_H =$ 440 and 455°C, respectively; the corresponding failure strains are 3.2 and 3%. For $t_H = 15$ s, the relative strengths are greater than or equal to 57% for hot-tool temperatures in the range 380–455°C, greater than or equal to 64% in the temperature range 395–440°C, and 74% at 410°C. The failure strains in the temperature range 380–455°C lie in the range 2.1–3.1%. For $t_H = 20$ s, the relative strengths are greater than 64% for hot-tool temperatures in the range 365–410°C, greater than or equal to 72% in the temperature range 365–395°C, with a maximum of 76% at 380°C. The failure strains in the temperature range 380–425°C lie in the range 2.6–3.1%. Thus, for a melt penetration of 0.13 mm, relative strengths of the order of 70–75% can be attained over hot-tool temperature ranges of 440–455, 398–425, and 365–395°C for heating times of 10, 15, and 20 s, respectively. The corresponding failure strains are of the order of 3%.

The filled symbols in Fig. 4, connected by thick lines, show weld strength (data from Table 4) for the higher weld penetration of 0.91 mm, as a function the hot-tool temperature for three heating times of 10, 15, and 20 s (indicated, respectively, by circles, triangles, and squares). A comparison of the data in columns five and six in Table 2 shows that, except at four test conditions ($T_H = 395$ and 410°C, $t_H = 15$ s; $T_H = 365$ and 380°C, $t_H = 20$ s), the weld strengths are systematically higher for the larger weld penetration of 0.91 mm. For a heating time of $t_H =$ 10 s, although the weld strengths are systematically higher at the larger weld penetration, the maximum achievable strengths are about the same. This is also true for $t_H =$ 15 s, although the maximum strengths are only marginally higher at the higher weld penetration. For a heating time of $t_H = 20$ s, the highest weld strength of 85% for a weld penetration 0f 0.91 mm is substantially larger than the highest strength of 76% attained at the lower weld penetration of 0.66 mm. This highest weld strength is of the same order as the highest weld strengths attained in 3.2-mm-thick specimens (Table 3) for a melt penetration of 0 mm. By and large, the failure strains track the weld strength; the failure strains are greater than 2.3% for relative weld strengths greater than 70%.

The following sequence of macrographs show the top and side views of the fracture surfaces of several welds for a heating time of 20 s, melt and weld penetrations of 0.13 and 0.91 mm, respectively, and a seal time of 10 s. Fig. 5a and b correspond to the weld made at $T_H = 380$°C, which has a relatively low weld strength of 59%. Clearly, the failure has occurred through the center of the weld, where the molten surfaces of the two specimens came together. Although material flowed outward, as evidenced by the material in the "bead," the hot-tool surface temperature was not sufficient for forming a strong weld. The top view (Fig. 5b) shows that while the weld "bead" has a large number of bubbles, the weld fracture surface has a relatively small number of bubbles, all of which are rather small. Notice from Fig. 5b that the molten and resolidified material in the weld zone is not of uniform thickness, being thin at the center and progressively becoming thicker at the ends where it merges into the bead. In comparison to PC and PBT welds [1,2], this thickness variation is more pronounced in PEI. At the higher hot-tool temperatures used for PEI, radiant heating of the lateral surfaces contributes to softening and melting of thicker layers near the specimen surfaces. The boundary between the heat-affected zone (HAZ) (lighter shade) and the base material (darker shade) which did not see a sufficient temperature increase is indicated by different shades caused by changes in the refractive index.

Fig. 6a and b show the top and side views of the fracture surfaces of the weld made at $T_H = 395$°C, which has a relatively high weld strength of 82%. The weld failed both in the resolidified weld zone as well as at the interface of the HAZ with the base material. The side view in Fig. 6b shows the material from the HAZ pulled away from the base material in regions close to the specimen surfaces. This

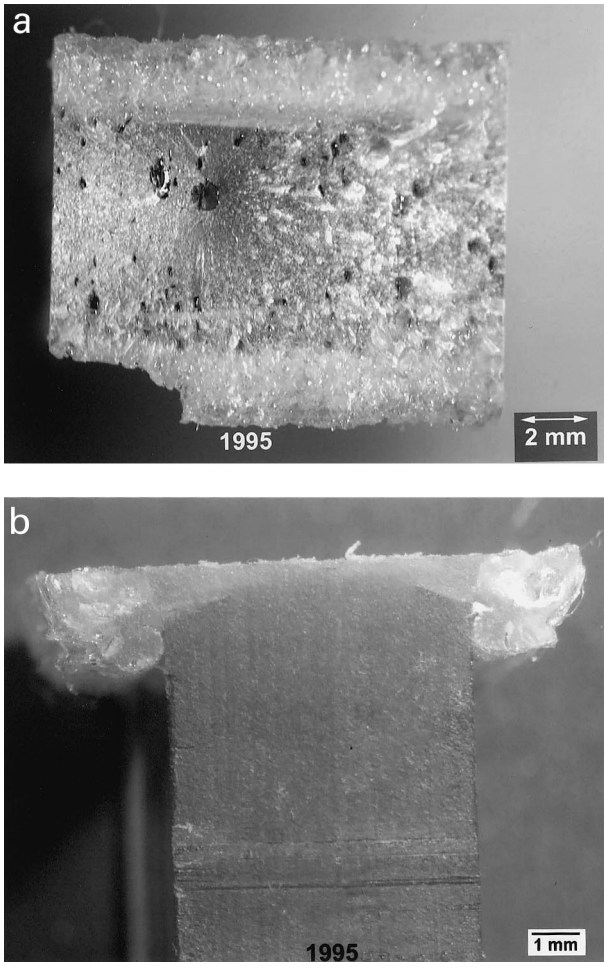

Fig. 5. Fracture surfaces of 6.2-mm-thick PEI specimens for hot-tool weld made at $T_H = 380°C$, a heating time of 20 s, melt and weld penetrations of 0.13 and 0.91 mm, respectively, and a seal time of 10 s. (a) Top view, and (b) side view.

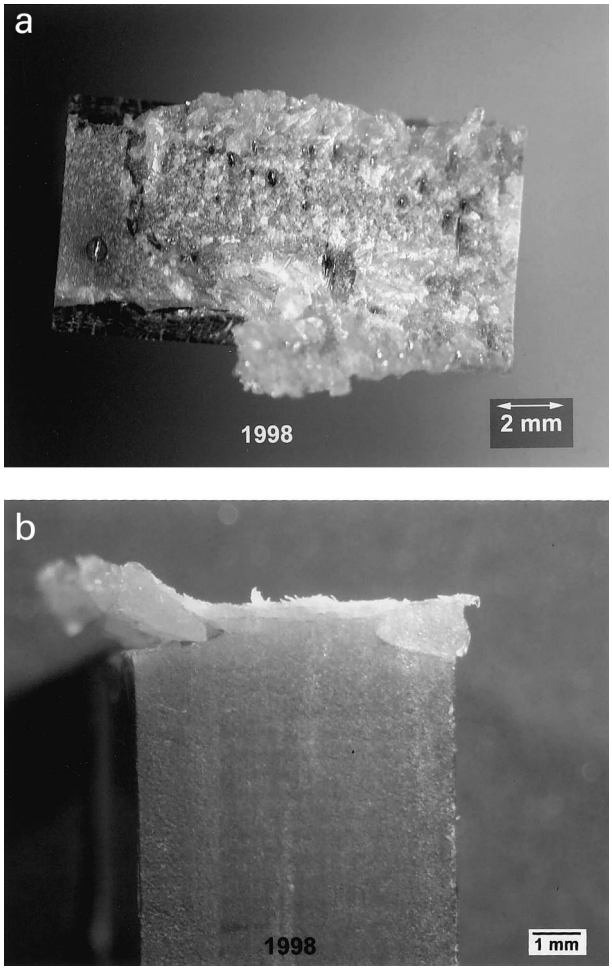

Fig. 6. Fracture surfaces of 6.2-mm-thick PEI specimens for hot-tool weld made at $T_H = 395°C$, a heating time of 20 s, melt and weld penetrations of 0.13 and 0.91 mm, respectively, and a seal time of 10 s. (a) Top view, and (b) side view.

material can be expelled outward during the tensile tests, leaving grooves on the sides that can be seen in the left region of the top view in Fig. 6a. In this specimen, most of the weld "bead" was ejected during tensile failure; the weld fracture surface has a relatively small number of bubbles, all of which are larger than in the specimen shown in Fig. 5a.

Fig. 7a and b show the top and side views of the fracture surfaces of the weld made at $T_H = 410°C$, which had the highest relative weld strength of 85%. In this specimen, the bulk of the failure occurred at the interface between the HAZ and the base material. Again, notice the grooves at the edges caused by this failure mode. The failure surfaces for this weld are very similar to those of the specimen in Fig. 6, except that the former has a larger number of bubbles on the failure surface. The failure surfaces for the welds made at $T_H = 425$ and 440°C are very similar to those for the ones made at 395 and 410°C.

Finally, Fig. 8a and b show the top and side views of the fracture surfaces of the weld made at $T_H = 455°C$, which has a relative weld strength of 70%. Here again, most of the weld bead was ejected during tensile failure. The main difference of the fracture surface for this specimen from those welded at lower temperatures is presence of large bubbles.

Thus, in the higher strength welds, all made at hot-tool temperatures in the range of 395–440°C, the failure occurs mostly at the interface of the HAZ with the base material. During failure in these welds, the thick HAZ at the edges is ejected out during failure, creating grooves near the specimen surfaces. At the higher weld temperature of 445°C, the fracture surface also has these edge grooves; the reduced strength (70%) is most likely caused by the presence of bubbles.

4.2.1. Effect of melt penetration

Strength and ductility data for 6.2-mm-thick PEI specimens, at a nominal strain rate of 0.01 s^{-1}, for a fixed weld penetration of 0.66 mm, at two melt penetrations of 0 and 0.13 mm, as functions of the hot-tool temperature and

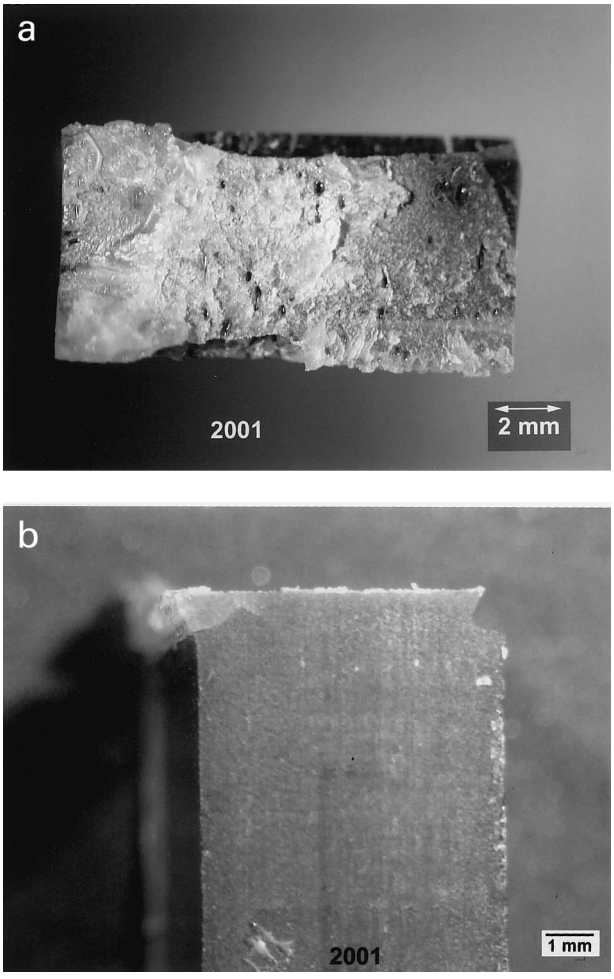

Fig. 7. Fracture surfaces of 6.2-mm-thick PEI specimens for hot-tool weld made at $T_H = 410°C$, a heating time of 20 s, melt and weld penetrations of 0.13 and 0.91 mm, respectively, and a seal time of 10 s. (a) Top view, and (b) side view.

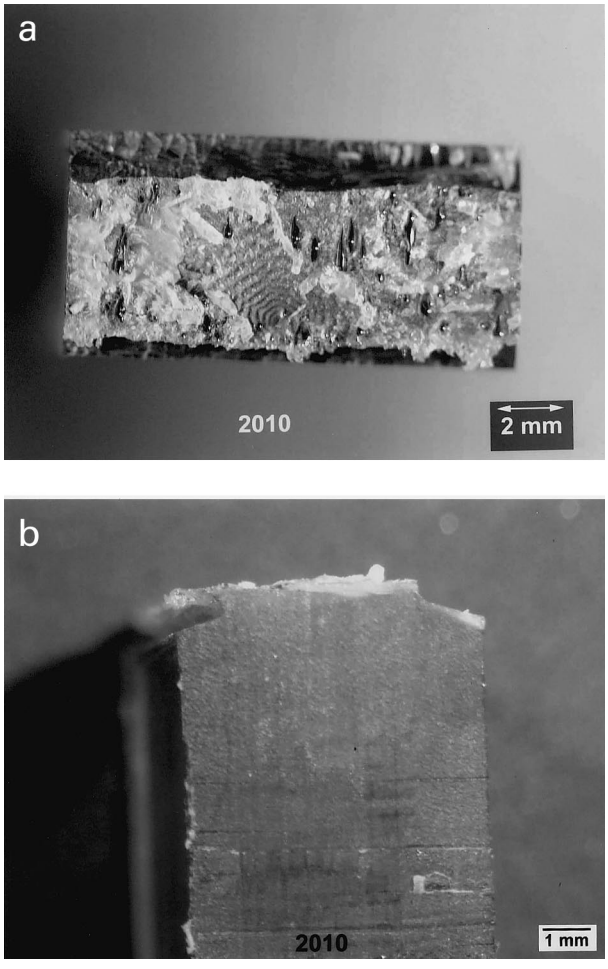

Fig. 8. Fracture surfaces of 6.2-mm-thick PEI specimens for hot-tool weld made at $T_H = 455°C$, a heating time of 20 s, melt and weld penetrations of 0.13 and 0.91 mm, respectively, and a seal time of 10 s. (a) Top view, and (b) side view.

the heating time, are listed in Table 5. The data for the higher melt penetration of 0.13 mm are from Table 4.

The variations of the relative weld strengths for $\delta_0 = 0$ and 0.13 mm are shown in Fig. 9 by the open and closed symbols, respectively. As before open circles, triangles, and squares correspond, respectively, to melt times of 10, 15, and 20 s. As in the 3.2-mm-thick specimen case, the relative weld strength is based on a resin strength of 111.6 MPa. For a heating time of $t_H = 10$ s, the relative weld strength is lower than 51% for all but four temperatures (410–455°C) with a maximum of 73% at 440°C. For $t_H = 15$ s, the relative strengths are greater than 55% for hot-tool temperatures in the range 380–455°C, greater than 70% in the temperature range 380–425°C, and 74–75% in the temperature range 395–410°C. The failure strains in the temperature range 380–455°C lie in the range 2.1–3.0%. For $t_H = 20$ s, the relative strengths are greater than 52% for hot-tool temperatures in the range 350–440°C, greater than 61% in the temperature range 365–425°C, greater than 70% in the temperature range 365–395°C, and 75–78% in the temperature range 365–380°C. The failure strains in the temperature range 350–425°C lie in the range 2.1–3%. Thus, for a melt penetration of 0 mm, relative strengths of the order of 75% can be attained over hot-tool temperature ranges of 395–425°C and 365–380°C for heating times of 15 and 20 s, respectively. The corresponding failure strains are of the order of 2.8%.

A comparison of Fig. 9 with Fig. 3 shows that, for 6.2-mm-thick specimens, the melt penetration appears to have a much smaller effect on weld strength (columns five and six in Table 5) than was observed in 3.2-mm-thick in specimens (columns five and six in Table 3).

4.2.2. Repeatability of test results

Most of the data in this paper were obtained from one test for each condition. To evaluate the repeatability of weld strength data, sets of five repeat tests were done on 6.2-mm-thick PEI specimens at each of the following conditions: at three hot-tool temperatures $T_H = 315$, 410, and 425°C for $t_H = 15$ s and $\delta_0 = 0$ mm; at three hot-tool

Table 5
Strength and ductility data for hot-tool welds of 6.2-mm-thick PEI specimens, at a strain rate of $\dot{\varepsilon} = 0.01\ s^{-1}$, as functions of the hot-tool temperature and the heating time, for two melt penetrations of 0 and 0.13 mm. The weld penetration was maintained at 0.66 mm and the seal time was kept constant at 10 s

Hot-tool temperature (°C)	Heating time (s)	Weld strength (MPa)		Relative weld strength[a] (%)		Failure strain[b] (%)		Δl (mm)		Differential penetration $\Delta\eta$ ($\Delta\eta_T$) (10^{-2} mm)	
		$\delta_0 = 0.0$ mm	$\delta_0 = 0.13$ mm	$\delta_0 = 0.0$ mm	$\delta_0 = 0.13$ mm	$\delta_0 = 0.0$ mm	$\delta_0 = 0.13$ mm	$\delta_0 = 0.0$ mm	$\delta_0 = 0.13$ mm	$\delta_0 = 0.0$ mm	$\delta_0 = 0.13$ mm
320	10	[c]	17.8	0	16	–	0.54	–	0.37	–	121 (135)
335	10	[d]	29.5	0	26	–	0.83	–	0.51	–	107 (123)
350	10	11.5	38.6	10	35	0.36	1.20	0.39	0.63	93 (109)	95 (111)
365	10	44.0	43.3	39	39	1.31	1.39	0.73	0.76	59 (75)	82 (98)
380	10	45.0	41.8	40	37	1.37	1.37	0.70	1.02	62 (80)	56 (74)
395	10	47.9	48.4	43	43	1.45	1.55	0.95	1.16	37 (55)	42 (60)
410	10	59.1	52.7	53	47	1.83	1.63	1.05	1.13	27 (45)	45 (63)
425	10	62.0	56.0	56	50	2.08	1.76	1.00	1.12	32 (52)	46 (66)
440	10	81.5	85.3	73	76	2.84	3.19	1.06	1.33	26 (46)	25 (45)
455	10	56.8	81.8	51	73	1.73	2.99	1.12	1.36	20 (42)	22 (44)
320	15	[d]	25.2	0	23	–	1.10	–	0.81	–	77 (95)
335	15	7.5	36.5	7	33	0.29	1.19	0.50	1.06	82 (100)	52 (70)
350	15	39.4	39.5	35	35	1.09	1.19	0.72	1.06	60 (80)	52 (72)
365	15	40.6	44.9	36	40	1.15	1.39	0.96	1.20	36 (56)	38 (58)
380	15	78.3	65.3	70	58	2.59	2.12	1.05	1.31	27 (49)	27 (49)
395	15	83.1	76.8	74	69	2.76	2.69	1.02	1.30	30 (52)	28 (50)
410	15	84.2	83.0	75	74	3.00	3.08	1.15	1.41	17 (41)	17 (41)
425	15	81.6	74.8	73	67	2.83	2.77	1.16	1.27	16 (40)	31 (55)
440	15	68.4	71.2	61	64	2.27	2.48	1.25	1.41	7 (31)	17 (41)
455	15	61.5	63.7	55	57	2.10	2.23	1.30	1.45	2 (28)	13 (39)
320	20	19.1	29.7	17	27	0.50	0.93	0.56	0.85	76 (96)	73 (93)
335	20	34.0	29.8	30	27	0.94	0.85	0.77	1.15	55 (77)	43 (63)
350	20	63.7	48.1	57	43	2.06	1.48	1.14	1.24	18 (40)	34 (56)
365	20	83.9	82.4	75	74	2.78	2.95	1.15	1.30	17 (41)	28 (50)
380	20	87.0	84.6	78	76	2.98	3.07	1.19	1.26	13 (37)	32 (56)
395	20	77.7	80.5	70	72	2.73	2.86	1.17	1.39	15 (41)	19 (45)
410	20	74.1	71.5	66	64	2.50	2.55	1.24	1.44	8 (34)	14 (40)
425	20	68.4	62.7	61	56	2.39	2.14	1.28	1.50	4 (32)	8 (36)
440	20	57.6	55.3	52	50	2.01	1.87	1.15	1.46	17 (45)	12 (40)
455	20	49.8	48.0	45	43	1.76	1.65	1.31	1.50	1 (31)	8 (36)

[a] $\sigma_0 = 111.6$ MPa.
[b] $\varepsilon_0 = 7.1\%$.
[c] Did not weld.
[d] Fell apart during welding.

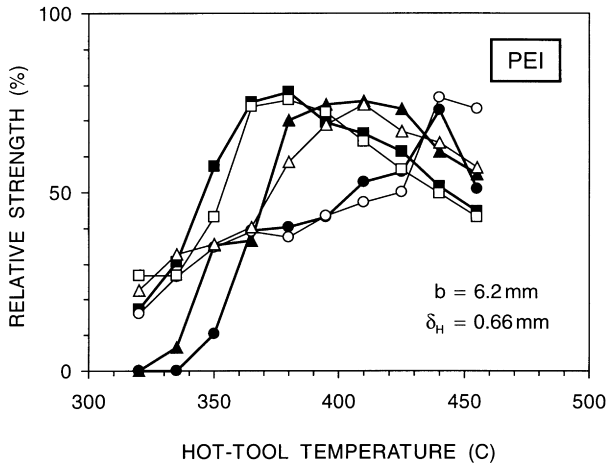

Fig. 9. Weld strength of 6.2-mm-thick PEI as a function of the hot-tool temperature, with the heating time as parameter. Circles, triangles, and squares correspond, respectively, to heating times of 10, 15, and 20 s. Open symbols (connected by thin lines) and solid symbols (connected by thick lines) correspond to melt penetrations and 0 and 0.13 mm, respectively. The weld penetration was maintained at 0.66 mm and the seal time was 10 s.

temperatures $T_H = 365$, 410, and 395°C for $t_H = 20$ s, and $\delta_0 = 0$ and 0.13 mm. The seal time was 10 s in all these tests. The data for these tests are listed in Table 6.

Mean values and standard deviations for these sets of five repeat tests are listed in Table 7. The highest average weld strengths of 88 MPa are obtained at the following three temperature, heating time, and melt penetration settings: $(T_H, t_H, \delta_0) = (410°C, 15\ s, 0\ mm)$, (380°C, 20 s, 0 mm), and (380°C, 20 s, 0.13 mm). At these three conditions, the standard deviation in weld strength is less than 3.5%. For all the conditions listed in Table 7, the standard deviations in strength are less than 7%. The average failure strains are about 2.5% with a standard deviation of less than 13%. The standard deviation in length changes is less than 7% for all the conditions listed in this table.

In contrast to welds of PC [1] and PBT [2], the data in Tables 6 and 7 show that both $\Delta\eta$ and $\Delta\eta_T$ are positive, thereby indicating that stops do come into contact during the final joining phase. This is also shown by the much tighter control of the final specimen dimensions, as reflected by Δl having a low variance in the range of 1.5–6.5%.

Fig. 10 shows the macrograph of the weld zone corresponding to conditions for the five repeat tests the data for which are summarized in the seventh row of Table 7 ($T_H =$ 365°C). The full view of the weld zone clearly shows that the HAZ is thinnest at the center, increasing to almost twice this thickness at the edges. This shape results from radiative heating of the specimen lateral surfaces while the specimen is in contact with the hot tool during the heating phase. At the end of the heating phase, this radiative heating results in the molten layer being thicker at the outer edges. The full view also shows bubbles distributed in the central plane of the HAZ. The close-up view shows these bubbles and the structure of the weld bead more clearly. The squeeze flow during the final joining phase squeezes the bubble trapped at the weld interface outward. This can be seen from the outer edges of the beads being bubble rich. Notice that away from the central HAZ core, the material flowing into the bead does not have any bubbles. This HAZ corresponds to the five tests in which a mean relative weld strength of 72% was achieved with a small variance of 3.4%.

Fig. 11 shows the macrograph of the weld zone corresponding to conditions for the five repeat tests the data for which are summarized in the eighth row of Table 7. This weld was made at a higher hot-tool temperature of $T_H =$ 380°C. In this weld, the bubbles in the HAZ are elongated by the squeeze-flow flow field. Also, during the last phase of welding shown in this figure, the central, bubble-filled HAZ core appears to "jet" through the bead, setting up a recirculating pattern in the bead. This HAZ corresponds to the five tests in which a mean relative weld strength of 79% was achieved with a small variance of 1.8%.

Fig. 12a and b show, respectively, the representative fracture surfaces for the repeat welds made at the conditions corresponding to those for the HAZs shown in Figs. 10 and 11. Both these weld fracture surfaces, made at a weld penetration of 0.66 mm, are similar to those for welds made at the higher weld penetration of 0.91 mm.

4.3. Comparison with vibration welds

The vibration welding of PEI is discussed in Ref. [5], where it is shown that maximum relative weld strengths of about 100% are achievable, that is, the static strength of PEI vibration welds can be as high as that of the resin. Thus, the maximum relative strength of hot-tool welds, 85%, is clearly lower than that for vibration welds.

The lower relative strengths of PEI hot-tool welds most likely result from absorbed moisture in the PEI specimens forming bubbles in the molten material. PEI is known to absorb more moisture than PC. This also explains why attaining high strengths in vibration welds of PEI requires high weld pressures at which bubbles are either not formed or cannot grow in size. Hot-tool welding with stops is a low-pressure process in which nucleation and growth of bubbles cannot be controlled.

5. Concluding remarks

It has been shown that strengths as high as 85% of the strength of the base resin can be attained in hot-tool welds of PEI specimens. For the weld process conditions studied, higher weld strengths in the 3.2-mm-thick material were obtained at the higher weld penetration of 0.66 mm and the lower melt penetration of 0 mm — the maximum strengths measured was 84%; the widest process window occurs for $t_H = 10$ s, $\delta_0 = 0.13$ mm, and $\delta_H = 0.66$ mm, for which relative weld strengths of about 70% can be obtained for hot-tool temperatures in the range $T_H = 380$–440°C. The

Table 6
Strength and ductility data for hot-tool welds of 6.2-mm-thick PEI specimens, at a strain rate of $\dot{\varepsilon} = 0.01\ s^{-1}$, as functions of the hot-tool temperature and the heating time, for a weld penetration of 0.66 mm. The seal time was kept constant at 10 s. Two melt penetrations of 0 and 0.13 mm were used. A set of five specimens were tested at each test condition

Hot-tool temperature (°C)	Heating time (s)	Weld strength (MPa)		Relative weld strength[a] (%)		Failure strain[b] (%)		Δl (mm)		Differential penetration $\Delta\eta(\Delta\eta_T)$ (10^{-2} mm)	
		$\delta_0 = 0.0$ mm	$\delta_0 = 0.13$ mm	$\delta_0 = 0.0$ mm	$\delta_0 = 0.13$ mm	$\delta_0 = 0.0$ mm	$\delta_0 = 0.13$ mm	$\delta_0 = 0.0$ mm	$\delta_0 = 0.13$ mm	$\delta_0 = 0.0$ mm	$\delta_0 = 0.13$ mm
395	15	81.5	–	73	–	2.35	–	1.11	–	21 (43)	–
395	15	89.7	–	80	–	2.33	–	1.11	–	21 (43)	–
395	15	83.1	–	74	–	2.76	–	1.02	–	30 (52)	–
395	15	90.7	–	81	–	2.42	–	1.09	–	23 (45)	–
395	15	82.1	–	74	–	2.33	–	0.98	–	34 (56)	–
410	15	88.5	–	79	–	2.31	–	1.23	–	9 (33)	–
410	15	84.2	–	75	–	3.00	–	1.15	–	17 (41)	–
410	15	90.4	–	81	–	2.35	–	1.15	–	17 (41)	–
410	15	91.5	–	82	–	2.36	–	1.10	–	22 (46)	–
410	15	85.4	–	77	–	2.34	–	1.03	–	29 (53)	–
425	15	83.5	–	75	–	2.38	–	1.20	–	12 (36)	–
425	15	82.1	–	74	–	2.32	–	1.16	–	16 (40)	–
425	15	79.5	–	71	–	2.36	–	1.24	–	8 (32)	–
425	15	81.6	–	73	–	2.83	–	1.16	–	16 (40)	–
425	15	83.6	–	75	–	2.45	–	1.24	–	8 (32)	–
365	20	71.6	85.2	64	76	2.10	2.28	1.07	1.30	25 (49)	28 (52)
365	20	84.8	75.0	76	67	2.34	2.30	1.10	1.33	22 (46)	25 (49)
365	20	78.0	79.1	70	71	2.28	2.32	1.07	1.32	25 (49)	26 (50)
365	20	83.9	82.4	75	74	2.78	2.95	1.15	1.30	17 (41)	28 (52)
365	20	79.0	80.8	71	72	2.31	2.29	1.09	1.29	23 (47)	29 (53)
380	20	86.7	89.5	78	80	2.26	2.27	1.19	1.30	13 (37)	28 (52)
380	20	86.7	89.4	78	80	2.33	2.37	1.14	1.35	18 (42)	23 (47)
380	20	89.2	88.1	80	79	2.34	2.35	1.14	1.36	18 (42)	22 (46)
380	20	89.8	88.5	80	79	2.32	2.24	1.14	1.32	18 (42)	26 (50)
380	20	87.0	84.6	78	76	2.98	3.07	1.19	1.26	13 (37)	32 (56)
395	20	85.4	85.6	77	77	2.31	2.38	1.22	1.32	10 (36)	26 (52)
395	20	91.9	83.4	82	75	2.29	2.34	1.23	1.38	9 (35)	20 (46)
395	20	77.7	80.5	70	72	2.73	2.86	1.17	1.39	15 (41)	19 (45)
395	20	83.3	85.8	75	77	2.38	2.34	1.24	1.36	8 (34)	22 (48)
395	20	87.1	76.4	78	68	2.36	2.20	1.17	1.37	15 (41)	21 (47)

[a] $\sigma_0 = 111.6$ MPa.
[b] $\varepsilon_0 = 7.1\%$.

Table 7
Repeatability of strength and ductility for hot-tool welds of 6.2-mm-thick PEI specimens as functions of the hot-tool temperature and the heating time. The weld penetration was maintained at 0.66 mm, and the seal time was kept constant at 10 s. Two melt penetrations of 0 and 0.13 mm were used. The averages and deviations are based on sets of five tests at each test condition (data from Table 6)

Hot-tool temperature (°C)	Heating time (s)	Melt penetration δ_0 (mm)	Weld strength (MPa) (percent relative weld strength[a])		Failure strain[b] (%)		Δl (mm)		Differential penetration $\Delta\eta$ ($\Delta\eta_T$) (10^{-2} m)
			Average	Standard deviation	Average	Standard deviation	Average	Standard deviation	Average
395	15	0	85.4 (77)	4.4 (3.9)	2.4	0.2	1.1	0.06	22 (44)
410	15	0	88.0 (79)	3.1 (2.8)	2.5	0.3	1.1	0.07	22 (46)
425	15	0	82.1 (74)	1.7 (1.5)	2.5	0.2	1.2	0.04	12 (36)
365	20	0	79.5 (71)	5.3 (4.7)	2.4	0.3	1.1	0.03	22 (46)
380	20	0	87.9 (79)	1.5 (1.3)	2.4	0.3	1.2	0.03	12 (36)
395	20	0	85.1 (76)	5.2 (4.7)	2.4	0.2	1.2	0.03	12 (38)
365	20	0.13	80.5 (72)	3.8 (3.4)	2.4	0.3	1.3	0.02	28 (52)
380	20	0.13	88.0 (79)	2.0 (1.8)	2.5	0.3	1.3	0.04	28 (52)
395	20	0.13	82.4 (74)	3.9 (3.5)	2.4	0.3	1.4	0.03	18 (44)

[a] $\sigma_0 = 111.6$ MPa.
[b] $\varepsilon_0 = 7.1\%$.

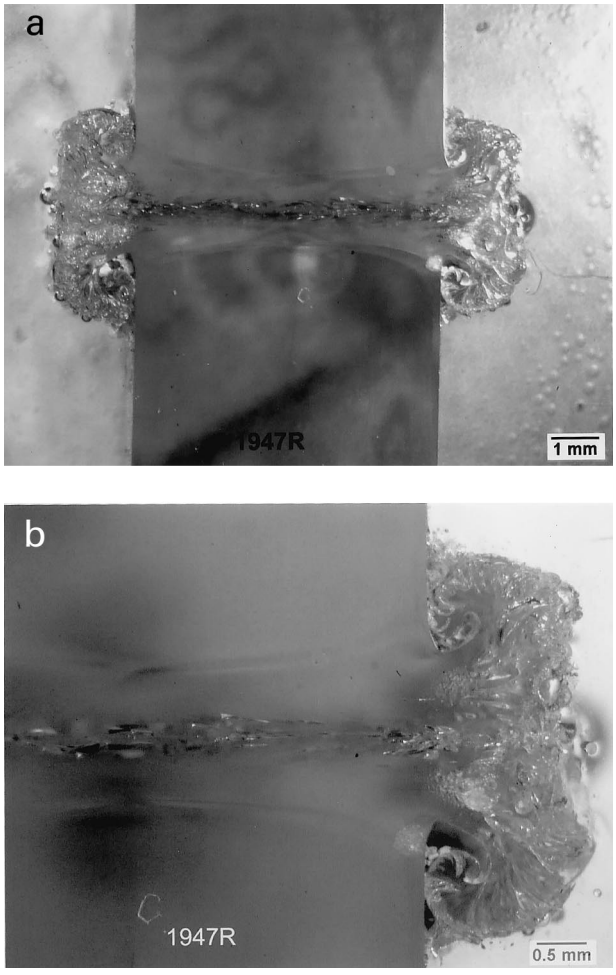

Fig. 10. Macrograph of weld zone in a 6.2-mm thick specimen welded at a hot-tool temperature of 365°C, a melt time of 20 s, melt and weld penetrations of 0.13 and 0.66 mm, respectively, and a seal time of 10 s. (a) Full view of HAZ and weld bead. (b) Close up showing bubbles in the HAZ core and detailed structure of bead.

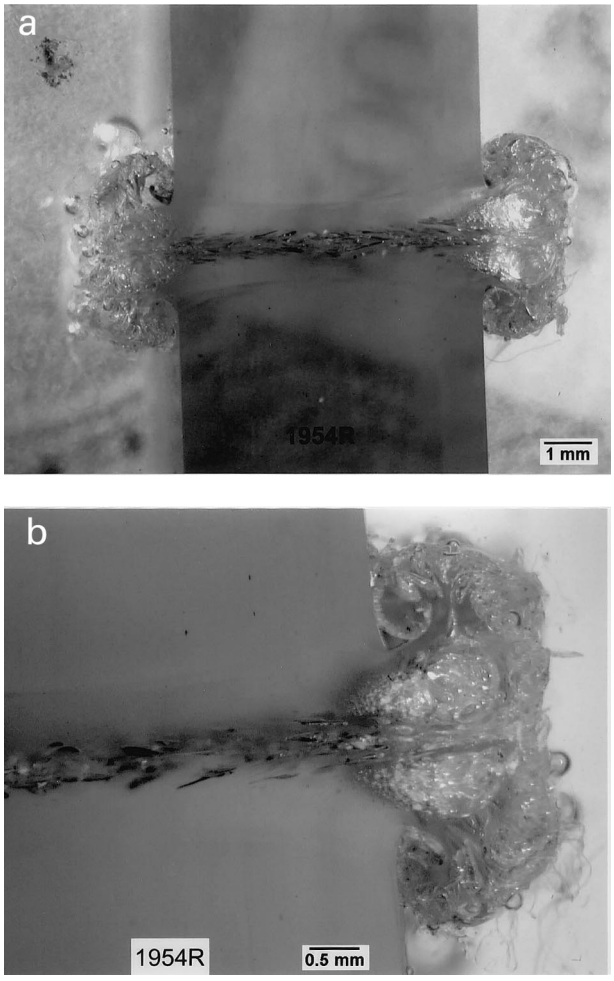

Fig. 11. Macrograph of weld zone in a 6.2-mm thick specimen welded at a hot-tool temperature of 380°C, a melt time of 20 s, melt and weld penetrations of 0.13 and 0.66 mm, respectively, and a seal time of 10 s. (a) Full view of HAZ and weld bead. (b) Close up showing bubbles in the HAZ core and detailed structure of bead.

highest weld strengths (85%) for the 6.2-mm-thick material were obtained at the highest weld penetration of 0.91 mm. For this weld penetration, relative weld strengths in the range of 80–85% can be obtained over a wide hot-tool temperature window of $T_H = 395$–440°C for melt and seal times of 20 and 10 s, respectively, and a melt penetration of 0.13 mm. The widest process window occurs for $t_H = 15$ s, $\delta_0 = 0$ mm, and $\delta_H = 0.66$ mm, for which relative weld strengths of 70–75% can be obtained for hot-tool temperatures in the range $T_H =$ 380–425°C. A higher weld penetration and a lower melt penetration appears to result in a higher weld strength. An increase in the heating time appears to reduce the hot-tool temperature required for obtaining high weld strengths.

The highest hot-tool weld strengths of about 85% are substantially lower than the 100% strength that has been demonstrated in vibration welds of this material. This reduced weld strength is most likely related to the morphology near the weld bead and the properties of the material in the HAZ, resulting in the observed edge grooves on failure surfaces, and to the absorbed moisture forming bubbles. Such grooves are not present in failure surfaces of PC and PBT welds. Note that bubbles do not appear to have a large affect on the strengths of PC hot-tool welds [1]. But PEI is known to absorb more moisture than PC. It is possible that, as in PC [1], higher weld strengths can be achieved by welding dried PEI specimens. Hot-tool welding can be used to weld PEI to PC and PBT [6].

Most of the data in this paper were obtained from one test per weld process condition studied. While such data do not provide information on repeatability, they are useful for an initial mapping of weldability over a wide range of weld process conditions. Repeatability studies show that high average weld strengths with low variance can be achieved

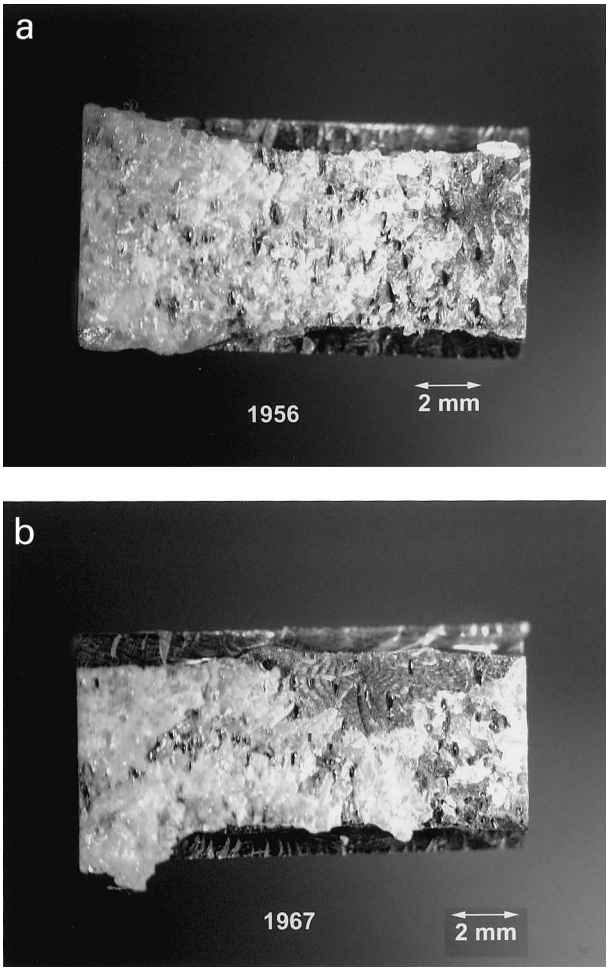

Fig. 12. Fracture surfaces of 6.2-mm-thick PEI specimens for hot-tool welds made at (a) $T_H = 380°C$, and (b) $T_H = 395°C$. In these welds, the melt time was 20 s, the melt and weld penetrations were 0.13 and 0.66 mm, respectively, and the seal time was 10 s.

in 6.2-mm-thick specimens. While hot-tool welding can produce strong welds, it requires careful dimensional and hot-tool temperature control, and a continuous cleaning of the hot-tool surface. In contrast, it is much easier to control the weld processing conditions in the vibration welding process.

Careful measurements of the differences between the initial and final lengths of specimens have not completely been reconciled with the differences expected on the basis of the machine stop settings. This discrepancy may either result from inaccuracies in the machine or from an inadequate analysis of thermal expansion effects. The length change data in this paper provide information for a more careful analysis of this welding process. The apparent variability of this welding process points to the need for more data at each test condition for a better mapping of the optimum welding conditions.

Acknowledgements

This work was supported by GE Plastics and the NIST ATP Project: Engineering Design with Injection-Molded Thermoplastics. The contributions of K.R. Conway, who carried out all the tests, and the inputs of L.P. Inzinna are greatly appreciated.

References

[1] Stokes VK. Polymer 1999;40:6235.
[2] Stokes VK. Polymer 2000;41:4317.
[3] Stokes VK. Polymer 1993;34:4445.
[4] Stokes VK. Polym Engng Sci 1997;37:692.
[5] Stokes VK. Polym Engng Sci 1988;28:998.
[6] Stokes VK. Polymer 1998;39:2469.